Driftwood and Hybrid Debris Barrier Interactions: Process of Trapping and Prevention of Releases during Overtopping

Toshiyuki Horiguchi, Guillaume Piton, Muhammad Badar Munir, Vincent Mano

INTERPRAEVENT 2021 – Norway

14th Congress INTERPRAEVENT 2021
Norway – Paper
www.interpraevent.at

Driftwood and Hybrid Debris Barrier Interactions: Process of Trapping and Prevention of Releases during Overtopping

Toshiyuki Horiguchi[1], Guillume Piton[2], Muhammad Badar Munir[3], Vincent Mano[4]

Keywords: debris flood, hybrid barrier, open Sabo dam, trapping effect, Discrete Element Method

Abstract

This study presents a new concept of debris barrier based on an experimental application to the Combe de Lancey stream (Villard-Bonnot, France). In 2005, 20,000 m^3 of gravels and large wood (LW) were transported and deposited. A debris basin was designed to trap sediment and LW supplied by extreme events while letting routine bedload transport to pass through. Here, hybrid barrier was successfully tested to achieve this dual objective. A short description of the catchment and proposed barrier is presented. Its trapping efficacy was also examined with a small-scale model. These laboratory observations were used to calibrate a numerical Discrete Element Model that to study processes driving LW entrapment and release. It highlights that a high accumulation of LW may occur on barriers. When water overflowed the barrier above a critical depth, the overtopping of massive LW was observed. To prevent it, a rack was tested and proved sufficient.

Introduction

During extreme debris flow and debris flood events, large wood (hereafter, LW), i.e., wood pieces longer than 1 m and thicker than 0.1 m, are often recruited along with high volumes of sediment. Such wood- and sediment-laden high discharges regularly damage downstream settlements. Closed Sabo dams had long been used as a preferred counter-measure for trapping sediment (Mizuyama 2008). However, a lot of LW may overflow such structures during disastrous events (Piton and Recking 2016). More recently, open Sabo dams, i.e., permeable structures, are increasingly implemented. They are supposed to possess better selectivity on sediment trapping, better trapping efficacy of LW and lower maintenance cost because of their ability to transfer fine sediment naturally (Shima et al. 2016). However field surveys report that some structures did not work as expected, e.g., slit dams did not self-cleaned because of large wood jamming at the openings (Mizuyama 2008). Although debris basins are created mainly for sediment trapping, LW regularly

[1] Dr., National Defense Academy, Japan, (debrissegregation@gmail.com)
[2] Dr., Univ. Grenoble Alpes, INRAE, ETNA, France
[3] Univ. Grenoble Alpes, INRAE, ETNA, France
[4] Dr., ARTELIA Eaux Et Environnement, France

affects the functionality of these hydraulic structures (Shima et al. 2015, Piton and Recking 2016). LW may be trapped by hydraulic structures during the rising limb of hydrograph, disrupting its functioning. In addition, a massive part of LW may eventually be released by overtopping the structures.

This paper is based on a case study of the Ruisseau de la Combe de Lancey, located in the Isère valley, north of Grenoble (France). The stream's alluvial fan is fully occupied by the Villard-Bonnot municipality, particularly by an old paper mill where the development of a new residential area is in progress. Protection of the whole area is mandatory before the construction of new settlements. Past studies demonstrated that a retention basin was the best option (SOGREAH 2006). Its best location would be slightly downstream of the fan apex (Fig. 1a), where most of the deposit occurred in 2005 during a large flood. Designing a retention basin in a city center needed a detailed analysis which has been performed using small scale modelling (ARTELIA and IRSTEA 2018). A particular challenge addressed in this case study was to design a debris basin with robust functioning regarding capacity to transfer small events and prevention of LW overtopping. Piton et al. (2019) demonstrated that the selected design achieved satisfying sediment trapping efficacy.

The main objective of this paper is to examine trapping effect on LW by the barrier and the drivers of potential release of LW downstream. Two design events were tested in the small-scale model with different peak discharges. LW releases were observed during the higher peak discharge. A rack was added on the initial barrier to prevent the release (compare Fig. 1c & d) and it gave satisfactory results. After a short description of the case study, this paper first reports the small scale experiment results. These results were secondly used to calibrate a Discrete Element Model (hereafter, DEM) of the barrier to finally examine which parameters drive trapping and release of LW at a barrier through virtual repetitions of the flume experiment.

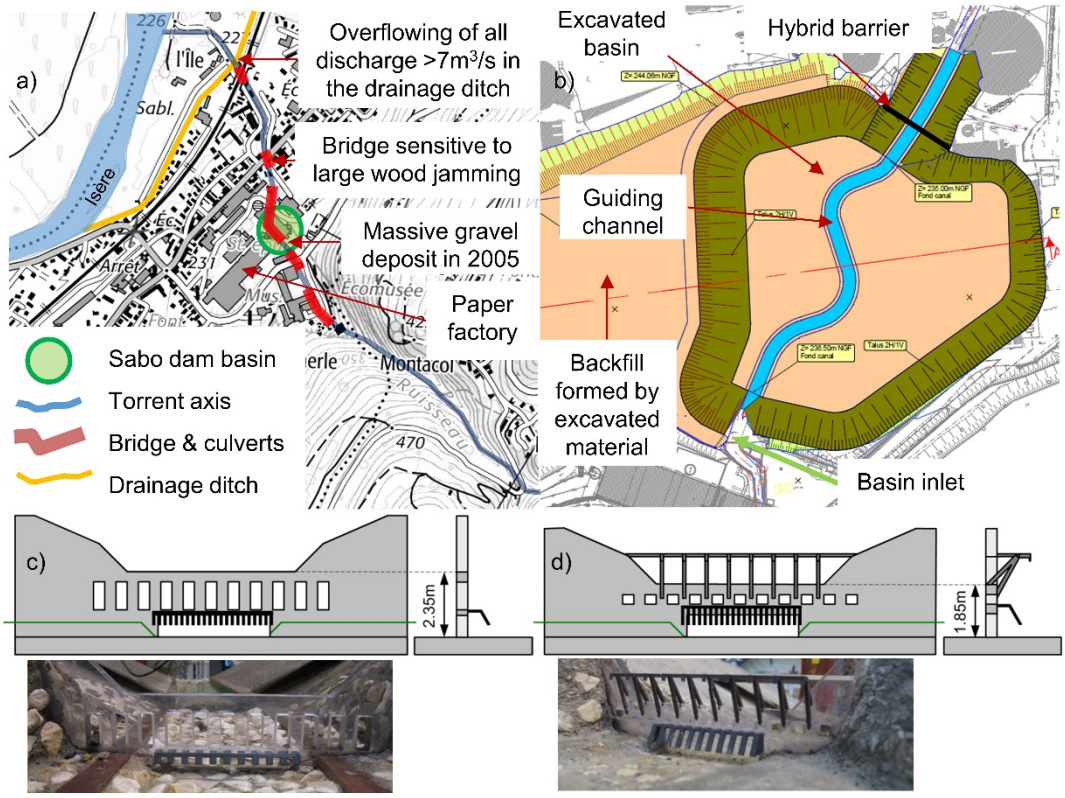

Figure 1 a) map of the alluvial fan and main hazardous points, b) zoom on the retention basin and location of the main structure, c) first version of the hybrid barrier called "initial barrier" (drawing and scaled version pictures) and, d) improved version of the hybrid barrier called "improved barrier" (drawing and scaled version picture), structure lowered but equipped with a rack

Case study description

A full description of the rarely active, 18 km² catchment can be found in Piton et al. (2019). On Aug. 21st and 22nd, 2005, a long lasting flood transported and deposited 20,000 m³ of sediment onto the fan (Fig.1a). SOGREAH (2006) demonstrated that sediment and LW trapping was required to protect the village: downstream channel has insufficient hydraulic capacity and several bridges are prone to be jammed by LW. The debris basin should ideally be a large excavated basin located where debris deposition occurred in 2005 (Fig.1b). State-of-the-art hydrology enabled to define peak discharges: Q30years≈ 22 m³/s and Q100years ≈ 35 m³/s (SOGREAH 2006). The extraordinary long duration of the 2005 event was studied by Piton et al. (2019). They concluded that although the peak discharge was close to the 1:30 years return period, the bivariate statistical analysis of peak discharge and duration falls within the ±20% uncertainty range around the 1:100 year exceedance probability when accounting for decreasing discharge for increasing duration, i.e., the bivariate time return for both events was somewhat equivalent. Several flood scenarios were thus defined: (i) the 2005's disaster, hereafter referred to as "Q100L" with peak discharge 22 m³/s and a long duration of 30 h, as well as (ii) a shorter and more typical 1:100 years return period of debris flood, "Q100s": peak discharge 35 m³/s and duration of 18 h. Both events were tested using small scale model and then reproduced in DEM.

Other events with higher solid concentration, bigger sediment supply or coarser grain sizes were also tested in the flume to check the robustness of the structure functioning regarding varying events or return periods. The barrier proved very robust to the variability of events (Piton et al. 2019).

Flume experiments: model description

A 1:40 scaled model of the basin with a length and width of about 3.0 m was built (Fig. 1c-d). A 56 mm high hybrid barrier was installed at the outlet. Its detailed design is presented in Piton et al. (2019). The sediment mixture was composed of poorly sorted sand and gravels of diameter 1-13 mm. Multiple high waterfalls and pools are located in the gorge immediately upstream of the alluvial fan. Flow energy in this area is capable to break tree crowns, trunks and root wads. Field survey demonstrated that only LW of a few meters, i.e., no whole trees, was found approaching the fan. Archived pictures from 2005 and another event in 1939 confirmed this point. LW was consequently added to both runs as mixture of thin (diameter: 1 mm, length: 40 mm, number: 764) and the thick wooden logs (diameter: 5 mm, length: 40 mm, number: 122). Logs were fresh branches and needles of pine tree. LW was not soaked prior to experiment. LW was introduced manually during the rising limb of the hydrograph, starting when discharge overpassed the 10 years return period (15 m^3/s at prototype scale).

Flume experiments: model results

Flow depth was measured directly upstream of the barrier. It reached hw = 81 mm above bed at peak flows during run Q100L and hw = 86 mm during run Q100s. In both runs, sediment filled the basin progressively. The deposited front eventually reached the barrier at the end of the runs demonstrating full entrapment of sediment. At the beginning of both runs LW was efficiently transported and accumulated against the barrier. It progressively clogged the orifices thus increasing water depth at the barrier; as a consequence the flow rapidly overflowed the spillway.

As shown in Fig. 2a, nearly all LW was trapped by the barrier during run Q100L, even at peak discharges (22 m^3/s at prototype scale). LW formed a thick jam, tightly entangled at the barrier and kept piling up even though overflowing depth (20-25 mm) was much higher than average log diameter (1 or 5 mm). Under such conditions, the average velocity of the approaching flow was 0.10 m/s.

The close packing against the barrier was also observed during the first steps of run Q100s. The cross sectional average velocity was approximately 0.17 m/s. When discharge approached 34 m^3/s at prototype scale, i.e., nearly peak flows of 35 m^3/s, most of the LW jam was suddenly released in two bursts (Fig. 2d, f & h).

Such sudden releases of most of LW should be prevented because bursts of LW flowing in congested mode increase dramatically the likelihood of bridge jamming (Gschnitzer et al. 2017). An improved design with a rack added on the spillway was thus proposed (compare Fig. 1c for initial barrier and Fig. 1d for improved barrier). Racks on open SABO dams have usually an angle below 90° with horizontal (Piton & Recking. 2016). This enables

drag forces to push LW forward, thus giving room to flow to pass through the rack. However, it somehow prevents the tight entanglement between pieces and the barrier, which, in the present case, is desirable because it holds the LW in the structure. Therefore, the rack was designed with a negative slope (angle with horizontal 113°, see Fig. 1d) with sort of hooks on top. Its function is to keep LW in the basin even when water depth overtopped it. The negative slope angle has the twofold advantage to better stabilize the LW jam and to have a 20% higher surface, thus hydraulic capacity, than a vertical structure.

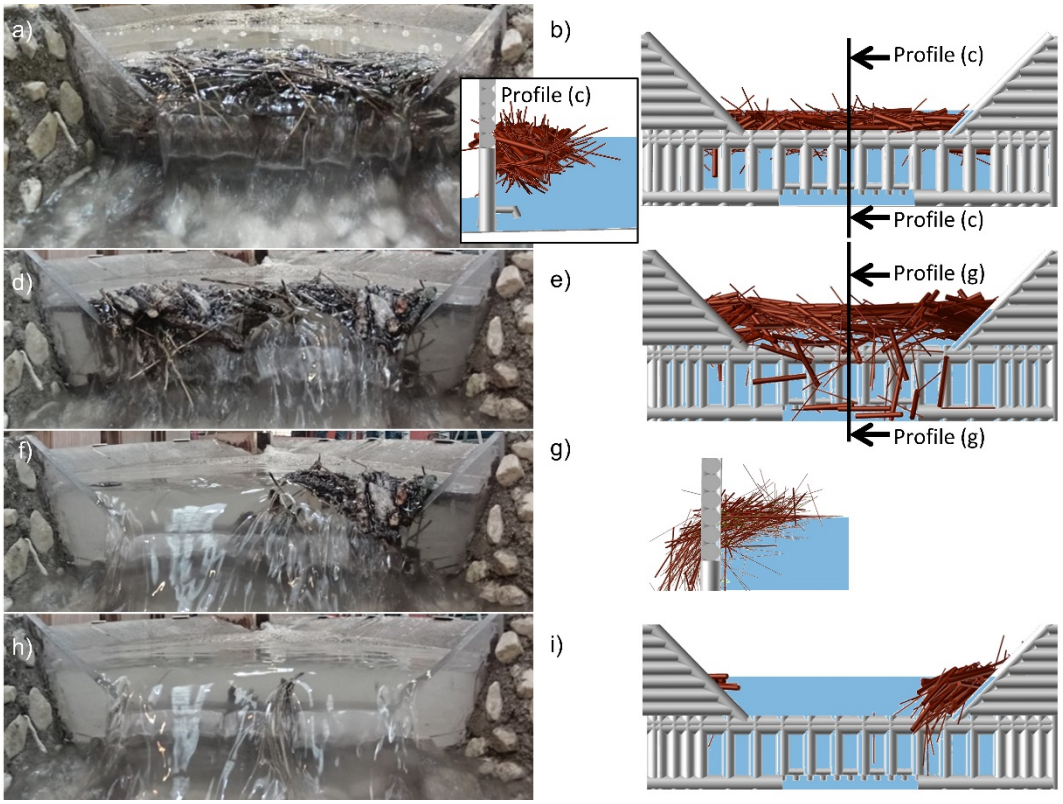

Figure 2 a) LW accumulation at the peak flow for the run Q100L, overflowing but no overtopping of log pieces, b) same situation modelled by DEM with linear free surface model, c) side view of image (b), d) LW accumulation just before release during run Q100s, e) starting of release during run Q100s modelled by DEM with horizontal free surface model, f) more than half of the accumulated wood was released, fast flow overtopping the barrier, g) side view of image (e), h) full release of floating elements in run Q100s and i) same situation modelled by DEM

Run Q100s was repeated with the improved barrier demonstrating that although a few pieces eventually passed through the rack, no more massive releases were observed and trapping conditions became satisfactory.

DEM analysis: model description

A numerical analysis was performed to understand the process of LW over topping at the barriers. It was calibrated on the small-scale model and then a parametric study was performed. The coupled DEM-fluid model developed by Horiguchi et al. (2015) was used to reproduce the initial and improved barriers (Fig. 3a & c). Logs were computed as cylindrical elements with same size as LW used in the flume experiment. The model solves

the Newton equations for LW, including drag forces. The flow model is a simplified fluid dynamics model where the free surface profile is forced according to measurements performed in the flume. Two free surface models were used: in a first step, the free surface profile was simplified as horizontal until the barrier (Fig.3b). In a second step, a linearly decreasing free surface profile was incorporated (Fig. 3d). In the present work, velocity is uniform in the section, computed based on water discharge and wetted section and sediment is not included.

DEM analysis: parametric sensitivity analysis

Run Q100L was repeated only for the initial barrier. Run Q100s was tested for both the initial and the improved barrier (Table 1). Logs were initialized in random arrangement in the reach immediately upstream of the barrier. The approaching flows dragged the logs toward the barrier and reproduced their entanglement (Fig. 2).

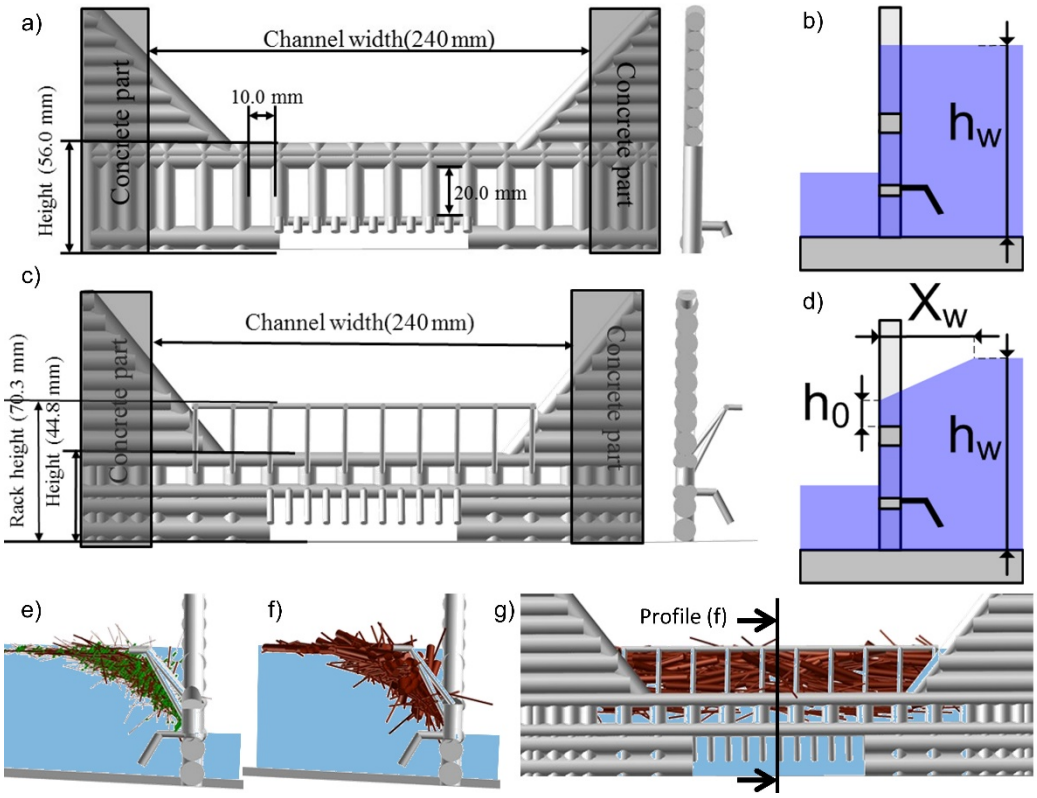

Figure 3 a) upstream and side view of the initial barrier, b) concept of simplified hydraulic free surface longitudinal profile with horizontal hypothesis, c) upstream and side view of the improved barrier, d) concept of longitudinal profile of hydraulic free su surface with linear hypothesis, e) side view of contact points within the accumulation for run Q100s, f) side view of accumulation, trapped by improved design for same instant and, g) downstream view for same instant.

As shown in Figure 2, the numerical model accurately reproduced the accumulation arrangement. The overtopping of LW for run Q100s occurred first centrally and secondly near wings, consistently with flume experiment. However, the lack of overflowing during run Q100L was correctly reproduced for water depth hw ≤ 76mm, for hw>76mm LW

overtopped the barrier (Table 1) when using the horizontal flow model, i.e., for a water depth 4 mm lower than in the flume. A parametric analysis with virtual runs (herein, called V_Q**) was undertaken to find how to improve the model. Numerical values of tested parameters are provided in Table 1. The next section describes the results qualitatively.

Table 1 Analysis case and outline of result

Run name	Barrier design	h_w water height [mm]	V_w water velocity m/s	ρ_w (LW density)	Objective of the run	Outline of result
Q100L low	Initial	66-76	0.10	0.5	*Calibration: Check consistency of DEM with flume*	*DEM similar to flume*
Q100L	Initial	77-81	0.10	0.5		*DEM overtopping of LW: inconsistent with flume*
Q100s	Initial	86	0.17	0.5		*DEM similar to flume*
V_Q100L.Fast	Initial	76	**0.17**	0.5	*Check influence of approaching mean water velocity*	*No influence (no overtopping)*
V_Q100s.Slow	Initial	**86**	0.10	0.5		*No influence (overtopping)*
V_Q100.Heavy	Initial	86	0.17	**0.7,0.9,1.06**	*Check how wood density influences wood overtopping*	*Density of less than 1.0 had no influence. Logs with density of 1.06 sink and cannot overtop the barrier.*
V_Q100L.linear	Initial	81	0.10	0.5	*Check influence of approaching velocity profile*	*DEM similar to flume*
V_Q100s.linear	Initial	86	0.17	0.5		*DEM similar to flume*
Q100s	Improved	86	0.17	0.5	*Validation: Check consistency of DEM with flume*	*DEM similar to flume*
V_Q100s.linear	Improved	81	0.10	0.5	*Check influence of approaching velocity profile*	*DEM similar to flume*

One possible hypothesis was that LW overflowed in run Q100s as well as in run Q100L because of the excess in drag force related to the approaching flow velocity. Two cross-control virtual runs were launched to check it. During run V_Q100L.Fast, flow velocity was forced as same value of run Q100s, nonetheless no log release was observed demonstrating that velocity is of secondary importance. A symmetric case was tested with run V_Q100s.Slow where velocity was decreased to the value of run Q100L, nonetheless LW were released as the previous result in Q100s. We concluded that although approaching velocity increases drag force and probably accumulation density, it is not the main triggering factor of the LW release.

Another possible parameter to drive LW overflow can be their floatability that is controlled by the density (Furlan, 2019). Runs with increased densities (Table 1 run V_Q100.Heavy) demonstrated that floating logs i.e. LW with density <1, gave similar results as in the previous cases with density of 0.5. Thus, density also appears of secondary importance in our case study with high amount of logs tightly entangled.

For the sake of simplicity, the free surface model was initially set horizontal until passing the barrier (Fig. 3b). This hypothesis could be responsible of our overestimation of LW overtopping by overestimating buoyancy force at the crest. Additional flume runs were performed to measure more precisely the free surface profile. It was later simplified in a linear model (Fig. 3d) with parameter Xw set at 0.033 m and h0 at 0.010 m. Once implemented in the DEM, it computed the overtopping of LW for hw = 81 mm consistent with the flume (Table 1 runs V_Q100L.linear). LW were also correctly released for run Q100s. DEM approach was then considered reasonably calibrated.

Finally, when the crest rack of the improved barrier (Fig. 1d) was numerically tested (Fig. 3e-g), it achieved similar results as the small-scale model, i.e., a few logs passed through the rack but the LW mostly remained trapped by the barrier.

Discussion: driving processes of LW accumulation and release

This section discusses the preliminary lessons learnt from this dual analysis with small-scale modelling and DEM. It is interesting to note that Furlan (2019) demonstrated that when flow depth is more than 1-2 times log diameters, LW is usually not trapped on reservoir dam spillways. Conversely, we observed LW jams are stable until flow depth reached 5-6 times log diameter. Compared to the experiments by Furlan (2019), we used higher volumes of LW and a time-dependent overflowing related to hydrographs. LW jams were progressive with partial passing through the openings. When trapped through openings, logs are very stables and become fixed points upon which the jam piles up. Friction between logs in the flume and in DEM, where friction angle between logs is set to 22°, stabilized the jam. DEM computes and enables us to draw contact forces, i.e., interactions between LW pieces. Very complicated chain force networks emerged when several logs slid and piled up on each other. Fig. 3e displays for instance a side view of the central barrier cross-section. Chain forces are highlighted by LW thickness: the thicker the log, the more numerous are contact points with other logs or with the barrier. The resulting load of LW on barrier had a downward direction. Further works should be dedicated to study the magnitude, location and direction of the resulting loading and stress concentration.

For run Q100s with the initial barrier, the accumulated LW overflowed the structure. Before accumulated LW burst and overtopped the barrier, flume experiment showed that LW slowly and progressively migrated over the barrier. Small rearrangements of LW resulted from distinct downward flow, increasing the accumulation compactness and pulling the logs towards the bottom and impacts of upstream approaching logs. The chain forces thus kept on varying randomly. Increase in flow depth also decreased LW contacts

and load transfer with the barrier due to LW buoyancy. At some point, friction between logs and load transfer on the barrier no longer exceeds buoyancy plus flow drag and the accumulation bursts downstream (Run Q100s: Fig. 2).

The rack on the crest prevents this progressive overtopping and rearrangement by providing solid supports to any LW approaching the crest. Massive amount of LW was thus gathered above the barrier. The rack also holds part of LW buoyancy force and drag force. Loading is different in both the initial and improved design. Further works will be dedicated to study load diagram, stress distribution as well as resulting forces and structural design.

It is worth stressing that simple cylindrical elements were used in both the small-scale model and the DEM to model LW for the site-specific reasons as explained above. In field applications where LW with branches, crowns and root wads may be encountered, one should expect higher stability of jams but also denser jam because of small particles like leaves and small branches, which can result in higher head losses and overtopping depth for same discharges.

Conclusion

We analyzed trapping effect of LW and its release at open Sabo dams. Results from a small-scale physical model enabled calibrating a DEM approach. In both models, it was observed that LW might accumulate in jams with thickness equivalent up to 5 times log diameters. Their entanglement, interactions between elements and with the barrier crest hold them upstream of the barrier. At some point, when discharge and head losses are such that flow depth over the crest reaches a critical value, LW jams may burst and be suddenly released. Adding a rack at the crest enabled to prevent such releases.

Acknowledgements

The authors would like to thank the Villard-Bonnot municipality for allowing the study results to be re-used in this paper as well as the two anonymous reviewers who provided very constructive comments and helped us improving this manuscript.

References

ARTELIA & IRSTEA. 2018. Etude de l'Aménagement d'une Plage de Dépôt sur le Torrent de la Combe De Lancey - Site des Anciennes Papèteries de Villard Bonnot - Rapport de Modélisation Physique. Ville de Villard-Bonnot.

Furlan, P. 2019. Blocking probability of large wood and resulting head increase at ogee crest spillways. PhD dissertation, EPFL (Lausanne) and IST (Lisboa), 160 p.

Gschnitzer et al. 2017. Towards a robust assessment of bridge clogging processes in flood risk management. *Geomorphology*, 279:128-140

Horiguchi et al. 2015. A Basic Study on Protective Steel Structures against Woody Debris Hazards. International *Journal of Protective Structures* 6:191–215.

Mizuyama. 2008. Structural Countermeasures for Debris Flow Disasters. *International Journal of Erosion Control Engineering* 1(2):38–43.

Piton et al. 2019. Design of a debris retention basin enabling sediment continuity for small events: the Combe de Lancey case study (France). Proc. 7th Int. Conf. on Debris-Flow Hazards Mitigation: Mechanics, Prediction, and Assessment, 1019-1026

Piton & Recking. 2016. Design of sediment traps with open check dams. II: woody debris. *Journal of Hydraulic Engineering* 142:1–17.

Shima et al. 2015. Consideration on boulders & members' interval of open type steel sabo dam for capturing debris flow. *Journal of the Japan Society of Erosion Control Engineering* 67(5):3-11

Shima et al. 2016. Prevention and mitigation of debris flow hazards by using steel open-type sabo dams. *International Journal of Erosion Control Engineering* 9(3):135–144.

Sogreah 2006. Etude de Diagnostic et d.amnagement Hydraulique du Bassin Versant du Ruisseau de la Combe De Lancey. Technical report. Commune de Villard-bonnot